IEEE Access
Multidisciplinary | Rapid Review | Open Access Journal

Received May 10, 2021, accepted June 23, 2021, date of publication July 15, 2021, date of current version July 22, 2021.

Digital Object Identifier 10.1109/ACCESS.2021.3097606

A Novel Grading System for Autism Severity Level Using Task-Based Functional MRI: A Response to Speech Study

REEM HAWEEL[1,2], AHMED M. SHALABY[1], ALI H. MAHMOUD[1], MOHAMMED GHAZAL[3], (Senior Member, IEEE), NOHA SEADA[2], SAID GHONIEMY[2], MANUEL CASANOVA[4], GREGORY N. BARNES[5], AND AYMAN EL-BAZ[1], (Senior Member, IEEE)

[1]Bioengineering Department, University of Louisville, Louisville, KY 40292, USA
[2]Faculty of Computer and Information Sciences, University of Ain Shams, Cairo 11517, Egypt
[3]Electrical and Computer Engineering Department, Abu Dhabi University, Khalifa City, Abu Dhabi, United Arab Emirates
[4]Biomedical Sciences, University of South Carolina School of Medicine Greenville, Greenville, SC 29605, USA
[5]Department of Neurology, University of Louisville, Louisville, KY 40292, USA

Corresponding author: Ayman El-Baz (ayman.elbaz@louisville.edu)

This work involved human subjects or animals in its research. The authors confirm that all human/animal subject research procedures and protocols are exempt from review board approval.

ABSTRACT Autism spectrum disorder (ASD) is a neuro-developmental disorder associated with impairments in social and lingual abilities. Failure in language development is variable in the ASD population and follows a wide spectrum. The autism diagnostic observation schedule (ADOS) is the current gold standard for diagnosing plus expert clinical judgment. Currently, studies aim to develop objective computer-aided technologies to diagnose autism with brain imaging modalities and machine learning. Task-based fMRI is a discriminating image modality that measures the functional activation of the brain. Computer-aided diagnosis systems aim to classify autistic subjects against typically developed peers despite the fact that autism is defined over a wide spectrum. Here, we propose a novel computer-aided grading framework in infants and toddlers (between 12 and 40 months) dependent on the analysis of brain activation in response to a speech experiment. First, brain activation responses are analyzed for 157 autistic subjects divided into three groups of: 92 mild, 32 moderate,and 33 severe as defined by ADOS calibrated severity score. Increased hypoactivation of the superior temporal cortex, angular gyrus, primary auditory cortex and cingulate gyri is exhibited with increasing autism spectrum severity. Less lateralization is also present when activation of the left hemisphere regions is recorded. Second, only these region of interest (ROI) areas are included for further local and global feature extraction in our ASD grading system. A comprehensive, two-stage system is developed using different classifiers. Four-fold cross-validation is adopted for testing. The first stage discriminates between moderate and the other two groups with an accuracy of 0.83 (sensitivity = 0.73, specificity = 0.83). Subsequently, a second stage classifies subjects as mild or severe autism with an accuracy of 0.81 (sensitivity = 0.81, specificity = 0.76). Finally, two validation techniques of synthesizing for oversampling and e of multiple random training and testing sets were adopted. The validation results proved the robustness of the proposed framework for an early computer-aided grading system to place subjects on the autism spectrum.

INDEX TERMS Autism, FSL, GLM, machine learning, RF.

I. INTRODUCTION

Autism spectrum disorder (ASD) is a neuro-developmental disorder characterized by impairments in social communication combined with language delay and repetitive behavior [1]. Many etiologies of autism are idiopathic, and affected individuals fall in a wide range of linguistic and intellectual defect severity [2], [3]. The common standard for ASD diagnosis employs a behavioral instrument such as the autism diagnostic observation schedule (ADOS) [4] along with, history and expert clinical judgement. ASD is generally diagnosed between the age of

The associate editor coordinating the review of this manuscript and approving it for publication was Jason Gu.

three to five years, coinciding with the emergent noticeable symptoms.

One of the most critical indicators of autism is the failure in language development, a variable spectrum in the ASD population [5]. Some individuals have minimal verbal ability while others have difficulties not significantly different to specific language impairment individuals. Nevertheless, others develop near-typical expressive language outcome [6]. Early diagnosis and intervention are crucial for better assessment and treatment to decrease symptom severity in autism. Such diagnosis can be investigated as early as 12–14 months old with the advent of brain image modalities such as structural magnetic resonance imaging (sMRI), functional magnetic resonance imaging (fMRI) and diffusion tensor imaging (DTI) [7]. The clinical diagnosis is stable by this time in development [8]. Such scans not only manifest the distinguishing brain structural but also adopting task based and resting fMRI characteristics which could function as early biomarkers of autism [9].

Task-based fMRI is adopted to measure blood oxygen level-dependent (BOLD) signals in all brain regions and their homogeneity in response to experiments in different domains [10]. Such fMRI task domains include language and auditory tasks, motor tasks, visual tasks, and basic social processing tasks [11]. Several fMRI studies of autism investigated autistic abnormal brain functional response to language comprehension in comparison to typically developed (TD) peers [12]. These studies [13]–[15] measured the sleep functional MRI response to a simple bedtime story on 40 autistic toddlers and 40 TD toddlers (ages ranging from 12–48 months). They revealed abnormal laterality patterns in autistic toddlers with hypoactivation of the left anterior portion of the superior temporal cortex (aSTG), whereas the normal expected dominant activation of the left hemisphere aSTG was present in TD toddlers. They also demonstrated that lateralization abnormality increases with age which suggests the importance of early treatment and intervention.

A review [16] of studies up to 2013 suggested a strong correlation between atypical lateralization and language impairment. They concluded attenuated left hemisphere activation and anomalous lateralization in the functional areas responsible for language and prelinguistics in individuals with ASD, specifically the fronto-temporal regions. One of their reviewed papers [17] indicated that this atypical lateralization exists at a very early age. High-risk ASD infants (6–12 months) exhibited a lower lateralized responses to speech sounds in contrast to the stronger lateralization present in low-risk peers. Similar results were provided by a review in [18]. Another meta-analysis in [19] reviewed fMRI studies of ASD through 2013. For the auditory and language tasks, ASD subjects have increased activation in the right precentral gyrus in contrast to decreased left activation compared to the normal activation in TD individuals. Also greater activation in the bilateral superior temporal gyri (STG) and greater activation of left cingulate gyrus was present in TD than in ASD subjects.

Lai *et al.* [20] investigated the feasibility of employing fMRI as an objective indicator of language disability in ASD. FMRI scans were acquired during a passive presentation of prerecorded parental speech alternating with periods of silence. The study included 15 TD subjects (mean age: 12.1 years, standard deviation: 4.3), 12 age-matched language-impaired autistic subjects (mean age: 12.4 years, standard deviation: 4.7), and additional 27 autistic children (mean age: 8.4 years, standard deviation: 3.1) who underwent imaging while sedated. Analysis was performed on two regions of interest: primary auditory cortex (PAC) and STG, which are known to be involved with language perception. No difference in the PAC activity between ASD and TD individuals were observed. However, differential STG activity was present in 83% of the awake ASD subjects and 96% sedated autistic subjects compared to TD controls. Positive BOLD responses (PBR) have been widely analyzed in fMRI studies in autism. However, negative BOLD responses (NBR) to language have been less studied in autism. One study [21] was small and included 12 ASD and 12 TD (mean age: 12.4, standard deviation: 4, range: 7–22 years). These researchers investigated NBR and found reduced activation and increased functional connectivity between the STG and NBR exhibited regions in ASD compared to TD subjects. A similar study is presented in [22]. They have included two matched groups of autistic and TD, each having 6 children (5 boys and 1 girl) aged from 3.8 years to 6.6 years. Their aim was to employ fMRI in exploring developmental speech delay in ASD. They detected bilateral symmetric activation in the STG, which was not present in ASD as they exhibited lateralized and reduced involvement of PAC.

As concluded from the literature on task fMRI analysis of autism, substantial activation differences between ASD and TD individuals are present as early as 12 months old and persist through adulthood. These findings suggest task-based fMRI as a valuable early indicator for autism, which could be further refined by investigating machine learning techniques in automated autism diagnostic tools.

Despite the fact that task-based fMRI can be considered as a potential autism biomarker, few attempts to deploy it for classification have been recorded; for its limited public availability compared to other scans. The commonly incorporated and widely available image modalities used for classification with machine learning approaches are structural MRI and resting-state fMRI [23]. Guillaume Chanel in [24] applied multivariate pattern analysis (MVPA) fMRI scans of two social stimuli experiments. Support vector machines (SVMs) and recursive feature elimination (RFE) were applied for classification. They recorded accuracies between 69% and 92.3% in classifying between 15 ASD and 14 TD subjects. Another attempt to classify children with ASD from task-fMRI scans is demonstrated in [25]. They examined various methods to train generalizable recurrent neural networks from small datasets. The classification accuracy ranged from 51.8% to 69.8% correct diagnosis of 20 ASD vs. 19 TD subjects. Li *et al.* [26] attempted to

utilize both the temporal and spatial information exhibited in task-based fMRI. They applied a sliding window method that calculates the mean and standard deviation to extract the temporal statistics. To capture the spatial information, they developed 3D convolutional neural networks (CNNs) that are fed with 2-channel images created by the sliding window. The mean F-scores in the proposed framework increased by 8.5%. A study in [27] proposed a pipeline based on task fMRI for predicting treatment of social responsiveness scale. They extracted brain features using general linear model (GLM). Various feature selection approaches and random forest (RF) classifiers were applied. Their study included 20 autistic children (mean age: 5.90 years, SD = 1.07 years; 7 females, 13 males). A recent study in [28] proposed global and local ASD diagnosis for toddlers by analyzing the Brainnetome atlas (BNT) with stacked nonnegativity constraint auto-encoder (SNCAE). The study achieved 75.8% accuracy for classifying between 30 ASD and 30 TD.

Previous fMRI studies performed experiments on adults between 19 and 53 years [24] and subjects with younger ages [25] (6.05 $\pm$ 1.24 years). Whereas our current study includes toddlers/infants from 12 to 27 months old (largest task based fMRI study to date) aiming for early analysis and computer-aided detection of autism. Moreover, previous studies primarily aimed to analyze or diagnose ASD in two groups of ASD or TD. Although such diagnosis is useful, it is not sufficient for identifying differences among subjects and locating them across the wide autism spectrum. To consider the aforementioned limitations, we have developed an autism severity analysis and grading approach to identify each ASD toddler on the autism spectrum as mild, moderate, or severe based on the ADOS calibrated severity scores (CSS).

This paper is a two-tier study. First, common activated brain areas in ASD children are detected, which are responsible for hearing in response to speech task composed of three audio stimuli. We analyze task fMRI scans of 157 subjects who underwent the same speech experiment and acquisition protocol. Studies in literature either use approaches including statistical inference and detection or machine learning diagnosis. To our knowledge, no studies have used the classification of task-based fMRI for autism guided by statistical inferences, which inspired us to propose the second part of this study. Our goal is to analyze the difference in activation between three levels of autism severity in infants/toddlers. An automated autism grading system was developed that employs the analysis results as a preliminary step to classification. The analysis is performed after dividing subjects into three groups of autism severity level: mild/non-ASD, moderate, and severe ASD groups, based on ADOS CSS. We match our results with the state-of-the-art literature.

As a first approach to incorporate different machine learning classifiers to grade autism severity [29], we conducted an initial pilot grading study on 39 young autistic children who underwent an audio hearing task. Best achieved accuracy was 72% using the RF and RFE on features extracted from the whole brain.

For the second proposed part of the study, our framework is designed to extract features based on the activated areas incorporated at this response to a speech task, proven by the analysis step. Also, as a contribution to the first grading approach, we have included more subjects with valid scans to the classification framework. Finally, we have conducted a more comprehensive feature extraction and classification framework to enhance the overall results.

II. MATERIALS

A. PARTICIPANTS

The dataset used for this study is obtained by ''Biomarkers of Autism at 12 Months: From Brain Overgrowth to Genes'' dataset, available at the national database for autism research (NDAR: http://ndar.nih.gov). It was collected between Aug 2007 and June 2014. These data were obtained from The National Institute of Mental Health (NIMH) Data Archive in accordance with the Archive's data usage agreement and with approval of the University of Louisville IRB (protocol #19.0668). The methods were carried out in accordance with the relevant guidelines and regulations. Informed consent was obtained from all subjects or, if subjects are under 18, from a parent and/or legal guardian. 639 subjects were included and tracked roughly every 12 months starting at 12 months and until 48 months old.

The dataset collection mainly contains Mullen scales of early learning, ADOS module 1,2 and toddler, genomics samples, sMRI (T1) and (T2), DTI, single-shell DTI, resting-state fMRI, task-based fMRI and some other reports. Each scan was performed on a various number of subjects. Six experiments were performed in this dataset collection: response to speech fMRI, word language fMRI, social orienting fMRI, emotion fMRI, resting fMRI, and gene expression analysis. In this paper, we analyze the response to speech recorded fMRI scans.

The data selection criteria for our study is designed to include the subjects that have sMRI, task-based fMRI for the speech experiment, and ADOS toddler module. We have visually validated all sMRI scans. Also, every fMRI scan has been validated to have 154 volumes and no clear artifacts. Since both sMRI and fMRI scans are not acquired at the same date, we have included subjects with no more than 6 months' time difference between both scans. After applying all exclusion criteria, we have included 157 subjects in our study, which is one of the most extensive task-based fMRI sample sizes of such a young age up to date (mean: 24.5 months and standard deviation: 7 months, range: 12–40 months). The calibrated severity score (CSS) calculated for the toddler ADOS module indicates the level of autism severity. Therefore, it was the ground truth for our study. The CSS is assigned a number between 0 and 10 calculated from raw total domain scores obtained by ADOS reports [4]. As shown in Table 1, it is divided into 3 classes: mild (CSS 1–4), moderate (CSS 5–7), and severe (CSS 8–10). According to

TABLE 1. Demographics and Mullen score variables of three test groups.

Group	Age in months	% Males	Expressive Language	Receptive Language	Visual Reception	Fine Motor
Mild/non ASD*	21.34 ± 7.1	63	49.75	50.88	54.47	55.75
Moderate**	22.47 ± 8.02	78	35.97	36.88	45.91	46.88
Severe***	27.49 ± 5.67	81	32.39	33.36	44.97	41.51

*Mild group (CSS=1–4) is a group (N=92) with most subjects judged not to be on the Autism Spectrum based on ADOS and clinical judgement.
**Moderate group (CSS=5–7) is a group (N=32) with most subjects judged to be on the Autism Spectrum based on ADOS and clinical judgement.
***Severe group (CSS=8–10) is a group (N=33) with most subjects judged to be on the Autism Spectrum based on ADOS and clinical judgement.

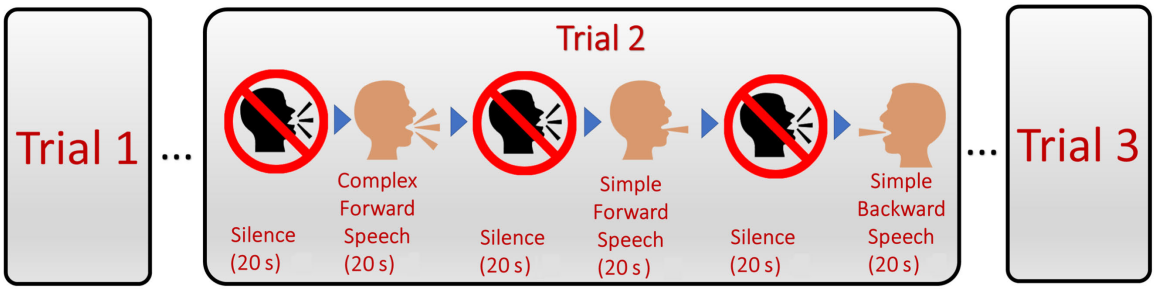

FIGURE 1. Illustration of task-based fMRI images which are acquired during a response to speech experiment that played an audio record of three stimuli: simple forward speech, complex forward speech, and backward speech which were alternating repeatedly along 6 min 20 seconds and separated by rest blocks.

TABLE 2. Scanner parameters for sMRI and fMRI scans. s: second, mm: millimeter, cm: centimeter, min: minute.

Scan type	Repetition time (TR)	Echo time (TE)	Flip angle	Bandwidth	Field of view	In-plane resolution	Slice thickness	Number of slices	Scan length
T1-weighted sMRI	6.5 ms	-	12	31.25 kHz	24 cm	1.1 mm	1.2 mm	170	7 min 24 s
Task fMRI	2.5 s	30 ms	90	70 kHz	25.6 cm	4 mm	4 mm	33	6 min 20 s

the CSS of the 157 included subjects, 92 are mild/non-ASD, 32 are moderate and, 33 are severely autistic.

B. TASK

Task-based fMRI images were acquired during the response to a speech experiment that played an audio record of three stimuli: simple forward speech, complex forward speech, and backward speech, which were alternating repeatedly along 6 minutes 20 seconds and separated by rest blocks. Figure 1 demonstrates the fMRI experiment design. All speech tasks were recorded by the same female speaker. The complex forward speech is a segment of a child's story with a comprehension level higher than 48 months old. However, simple forward speech contained uncomplicated language for toddler age. The backward speech is the reversed simple forward speech. Since participating subjects are infants and toddlers and the fact that they have fair language experience, there exists no significant difference between backward and forward speech tasks. Hence, in our analysis, we use all language tasks and compare them to rest blocks.

C. DATA ACQUISITION

Each subject had a corresponding structural (T1-weighted) MRI and task-based (T2*-weighted) fMRI, for the response to the speech experiment. A 1.5 T General Electric MRI scanner was used to acquire these scans after 15 minutes of natural sleep. Task fMRI images were acquired using echo-planar imaging. Parameters for both sMRI scan and fMRI are shown in table 2. As explained in Figure 2, FMRI session scan constitutes of 154 volumes. Each volume is combines slices acquired with the alternating in the plus direction slice acquisition pattern.

III. METHODS

Our study consists of two main parts: detection of significant activated brain areas for each study group in response to speech task, and the computer-aided diagnosis based on the resulted statistical inference of each group. Figure 3 explains our framework for both brain analysis and severity grading. First, we perform preprocessing to prepare fMRI images for first-level analysis using GLM. Then we apply group analysis to get statistical inference about the activated brain areas in each subject group and the difference in activation levels between them. The classification system depends on both the first level analysis per subject and the group analysis. The features for classification are extracted from the resulting GLM regressors and statistical maps of the first level analysis. Discriminant features are grouped over selected activated brain areas, which are guided by the group analysis.

A. DETECTION OF SIGNIFICANT ACTIVATED BRAIN AREAS

1) DATA PREPROCESSING

FMRI expert analysis tool (FEAT) [30] developed in fMRI's software library (FSL) [31] is utilized to perform the

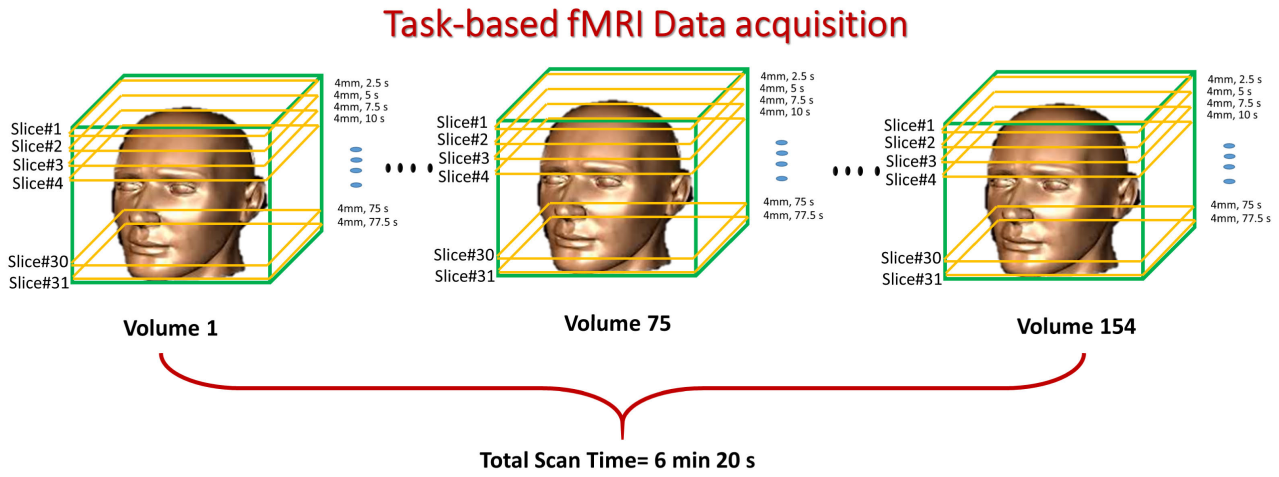

FIGURE 2. Data acquisition procedure during the response to speech fMRI task. Each scan consists of 154 volumes, each constructed by 31 slices scanned every 2.5 ms.

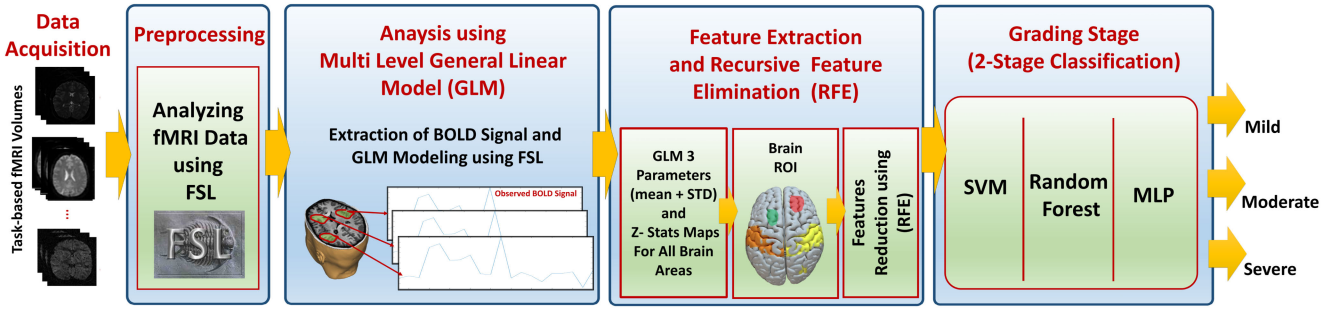

FIGURE 3. The proposed framework block diagram of using task-based fMRI images for grading autistic subjects into three severity levels. First, we perform preprocessing to prepare fMRI images for first level analysis using GLM. Then we apply group analysis to get statistical inference about the activated brain areas in each subject group and the difference in activation levels between them. The classification system on both the first level analysis per subject and the group analysis. The features for classification are extracted from the resulting GLM regressors and statistical maps of the first level analysis.

preprocessing pipeline. We have applied accordingly the following steps:

1) Slice time correction with interleaved order by shifting the time series of each slice to align all slices within a volume to a reference time point.
2) Motion correction to remove artifacts caused by the subject's motion in the scanner. Rigid-body transformations with 6 DOF is applied [32]. The residual motion remaining after motion correction was not substantial, so no subjects were excluded due to motion artifact.
3) Spatial smoothing using Gaussian window with full width at half maximum (FWHM) of 5mm, to enhance noise caused by high frequencies and enhancing low frequencies..
4) High pass temporal filtering at (100s) to correct for scanner drifts by removing low frequencies.
5) Brain extraction using BET on both sMRI and fMRI data, to remove all non-brain data such as the scalp. Every subject was visually validated, and subsequent adjustments were performed to carefully ensure accurate brain extraction.
6) Registration to standardize the fMRI brain images using fMRIB's linear image registration tool (FLIRT) [32] by applying two steps:1) register the functional volumes to their high-resolution anatomical sMRI scan, and 2) registration of the anatomical sMRI scan to MNI-152 space with a 12 DOF affine transformations [33].

2) GENERAL LINEAR MODEL

GLM has been the most convenient technique used for analyzing task-based fMRI in the past years [34]. It attempts to find a relation between the observed signal Y (dependent variable) and the set of predictors X (independent variables) as in eq.1. Such modeling is applied by tuning the parameter estimates β to find the best fitting lines.

$$y_i = \beta_1 x_{i1} + \beta_2 x_{i2} + \beta_3 x_{i3} + \ldots + \beta_j x_{ij} + \varepsilon_i \qquad (1)$$

For a group of N subjects, for each subject n, Y_n comprises a vector of T time points, X_n is the predictor design matrix and ϵ is the residual error. The GLM first level analysis for

$n = 1, \ldots, N$ is determined by:

$$\begin{bmatrix} Y_1 \\ Y_2 \\ \vdots \\ Y_N \end{bmatrix} = \begin{bmatrix} X_1 & 0 & \ldots & 0 \\ 0 & X_2 & & 0 \\ \vdots & \vdots & \ddots & \vdots \\ 0 & 0 & & X_N \end{bmatrix} \begin{bmatrix} \beta_1 \\ \beta_2 \\ \vdots \\ \beta_N \end{bmatrix} + \begin{bmatrix} \epsilon_1 \\ \epsilon_2 \\ \vdots \\ \epsilon_N \end{bmatrix} = X\beta + \epsilon \quad (2)$$

The first level parameter estimates are defined as:

$$\hat{\beta} = (X^T V^{-1} X) X^T V^{-1} Y \quad (3)$$

and

$$cov(\hat{\beta}) = (X^T V^{-1} X)^{-1} \quad (4)$$

where V is the covariance of ϵ. Similarly, the parameter estimates of the group-level GLM analysis are estimated by:

$$\hat{\beta_G} = (X_G^T V_G^{-1} X_G)^{-1} X^T V^{-1} Y \quad (5)$$

and

$$cov(\hat{\beta_G}) = (X_G^T V_G^{-1} X_G)^{-1}. \quad (6)$$

where X_G is the group-level design matrix, which separates the two groups (controls and patients), β_G is the vector of the group-level parameters and V_G is the covarince of η.

Following the estimation of the parameters β for each voxel, it is important to apply statistical tests to locate the significant activated voxels. Paired z-test [34], [35] is one of the most common statistical techniques used for determining the voxel significance. In addition, we express the statistical test result as a set of corrected P-values at each voxel. The GLM is a preliminary step to group analysis. Also the results of the GLM maps are utilized for classification. For more details about GLM parameter estimates, the reader is referred to [34]. Features are extracted from the e output β and z-scores.

3) MODELING OF BOLD SIGNAL

For each subject, we have applied first level analysis using FEAT. Adjustments to the FEAT parameters are applied prior to GLM employment. Speech events were modeled with the canonical double gamma haemodynamic response function (HRF) that is convoluted with the original waveform to blur and delay it to be matched and compared to the measured FMRI haemodynamic response. In order to support a better fit to the data, we applied temporal derivative to reduce unexplained noise and increase resulting statistical significance as well. FMRIB's improved linear model (FILM) prewhitening [36] was used to get valid and maximally efficient statistics. A contrast for each speech event, together with the contrast of the e of all three events, were calculated. The output of each subject's first level analysis and GLM calculations were used for getting the features for each subject. Mainly, we use the e β and e z-statistic of the three speech events after registering them to the standard space using FLIRT. In the following sections, we will discuss how to merge voxel values for each brain area after brain parcellation to get the features for the classifiers.

4) SIGNIFICANT BRAIN AREAS

We have compared the included three groups in our study by utilizing fMRIB's local analysis of mixed effects (FLAME1) [31] to perform high-level modeling. A two-tailed z-stat 3D file for each regressor in each group would result from the group analysis. We apply our analysis on cingulate gyri (CG), STG, PAC, and AG ROIs in the e of the three regressors. The positive 1-tailed z-stats are calculated then thresholded at voxel-wise FDR $q < 0.05$ on the selected ROI. Figure 4 and Figure 5 show the significant activation pattern for each of the three groups against rest periods.

B. COMPUTER AIDED DIAGNOSIS

We can infer mainly from our analysis results that there are activation differences in the STG, angular gyrus (AG), PAC,and CG between the comparison groups: mild/non-ASD, moderate,and severe, which conform with stated literature results. Hence, we have designed a computer-aided diagnosis framework that extracts features from these specific brain areas and applies different classification algorithms. We will discuss all details regarding feature extraction and classification in the following sections.

1) FEATURE EXTRACTION

We have examined various features extracted from the output regressors of the GLM analysis to test which features are more discriminating. First, global feature extraction for the whole brain is performed as the output from the first level FSL analysis. We examine two GLM output files: 1) the average of the three GLM regressors (parameter estimates) representing the three audio stimuli and 2) the average z-statistic of these regressors. Second, we perform local feature extraction by applying various calculations to the voxels included in each area to combine these features for each selected brain area. To group the average of the regressors grouped for each area, we have examined: 1) mean and standard deviation and 2) average of negative and positive values. To represent the average z-statistic grouping for each area, we have tested: 1) percentage of activated voxels, and 2) 6 bins histogram. The histogram is defined to calculate the percent of z-statistic intensity values within six intervals ($0 \leq |z| < 1, 1 \leq |z| < 2$, $2 \leq |z| < 3, 3 \leq |z| < 4, 4 \leq |z| < 5$, and $|z| \geq 5$). As shown in Figure 6, different feature vectors have been created for each GLM extracted feature file of the ROI brain areas. The final step examines each feature vector for the feature selection and classification stage.

Prior to classification, a feature selection step has been included to reduce the size and hence the dimension of the ROI extracted features. Recursive feature elimination (RFE) [37] is the feature selection algorithm applied in this study. Various models of the support vector machine and random forest classifier with are selected as classifiers to fit the selection model for included features. Four-fold cross-validation RFE experiment selecting important features is performed across train sets and validated over test sets

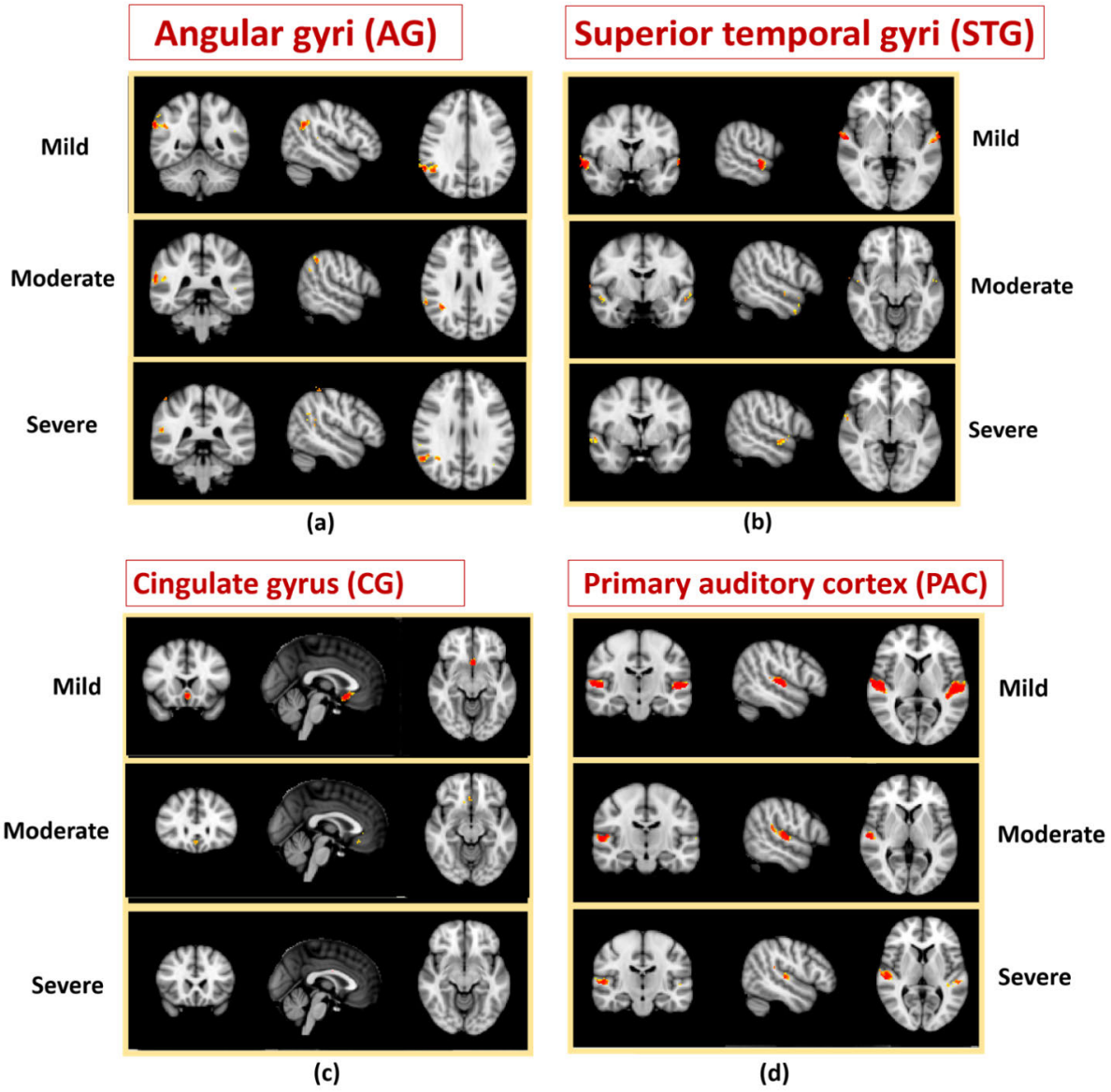

FIGURE 4. Activation in (a) AG, (b) STG, (c) CG and (d) PAC for each study group. We have compared the included three groups in our study by utilizing fMRIB's local analysis of mixed effects (FLAME1) [31] to perform high level modeling.

with multiple random runs. These models sort input features then the least important ones are recursively removed. In our framework, all RFE classifiers are run over 100 iterations calculating the selection frequency by each classifier. Afterwards, the features with higher selection frequency are selected for the overall classification stage for grading.

2) CLASSIFICATION

In this experiment, three different classifiers fed with each selected features vector are examined. The tested classifiers are support vector machine, random forest, and multi-layer perceptron (MLP), with randomly selected hyperparameters within defined ranges, on hundred runs. A fourfold cross-validation technique is performed to estimate the classification accuracies. We have tested each feature vector with all classifiers to check the best feature vector and best performing classifier for our data. As shown in fig. 7, a two-stage classification technique has been applied. First, each group is classified against the other groups. Second, a classification is applied between each pair of groups. Following each classification, we have applied a validation step to check the robustness of the classification accuracy and to avoid sampling bias.

IV. EXPERIMENTAL RESULTS

A. DEMOGRAPHICS AND MULLEN SCORES

Our study divided all infants and toddlers based on their ADOS CSS (Table 1). The mild group ultimately was judged

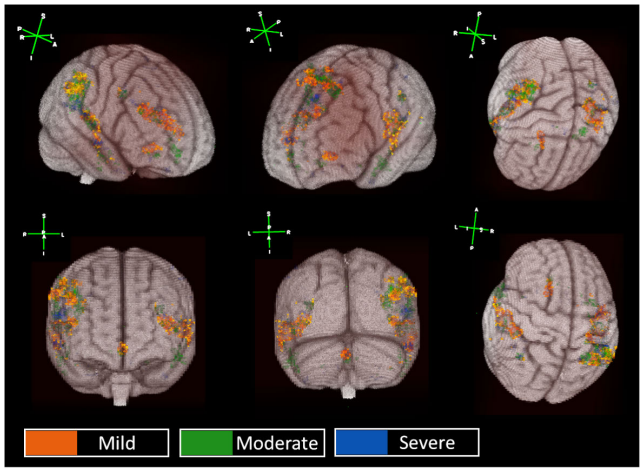

FIGURE 5. The 3D illustration for the results of group analysis.

to not be on the autism spectrum. This group is higher functioning with the highest T scores on Mullen expressive, Mullen language, Mullen visual response, and Mullen fine motor scales and nearly mimics those reported in TD subjects [38]. The Mullen expressive and receptive language scores and ages are not different between the moderate and severe ASD groups. Each of those scores represents a T score<40, which is 1 SD off the mean (Table 1).

B. CLASSIFICATION

At the first classification stage, we have classified each group against the remaining groups. Table 3 presents the accuracy, sensitivity and specificity of each group and the remaining groups. The best accuracy achieved for classifying between mild, moderate and severe against the remaining two groups are 73%, 84% and 83% respectively. The random forest classifier achieves better accuracy with our features.

TABLE 3. Accuracy, sensitivity and specificity of classifying between each group and the other groups.

	Accuracy	Sensitivity	Specificity	Best classifier
Mild-other	0.73	0.736	0.766	RF
Moderate-other	0.83	0.73	0.83	RF
Severe-other	0.83	0.875	0.826	RF

For the second classification stage, we have tested our classifiers to compare between (mild-moderate), (mild-severe) and (moderate-severe), in order to prove the uniqueness of each group based on fMRI parameters. Table 4 shows the best classification accuracy, sensitivity, and specificity for each pair without data balancing. We have classified (mild-moderate) with accuracy of 80%, (mild-severe) with accuracy of 80% and (moderate-severe) with accuracy of 78%. Best accuracies are still obtained by the RF classifier fed with the percentage of thresholded z-stat values, in each activated brain area, of the e z-stat image.

TABLE 4. Accuracy, sensitivity and specificity of classifying between each group pair.

	Accuracy	Sensitivity	Specificity	Best classifier
Mild-Moderate	0.8	0.79	0.88	RF
mild-Severe	0.81	0.81	0.76	RF
Moderate-Severe	0.77	0.77	0.76	RF

The distribution of the group sets is not balanced; 91 mild, 32 moderate, and 33 severe subjects. Hence, we have also tested the classification of the datasets after balancing our samples. Balancing was performed using subsampling. A matching size random samples is selected from the majority class to be classified with each minority class. Classifying after under sampling is performed between mild-moderate and mild-severe. Table 5 shows the maximum and e classification accuracies for both group pairs. To classify between mild and moderate, max accuracy is 0.79, and e accuracy is 0.75. To classify between mild and severe, maximum accuracy is 0.84, and average accuracy is 0.8. Fig. 8 demonstrates the confusion matrix of true and predicted labels of classifying each balanced group pair.

TABLE 5. Accuracy, sensitivity and specificity of balanced classification between each group and the other groups, using under sampling.

	Max accuracy	Sensitivity	Specificity	Avg. accuracy
Mild-Moderate	0.79	0.77	0.827	0.75
Mild-Severe	0.84	0.84	0.82	0.8

C. VALIDATION

We have developed a comprehensive validation stage. Each classifier has been run with random selection for training and testing by 4-fold cross-validation over 100 run. Maximum and average accuracy were calculated. For mild against the remaining groups, maximum accuracy is 71%, average is 68%. For Moderate against the remaining groups, maximum accuracy is 83%, average is 80%. For Severe against the remaining groups, maximum accuracy is 82%, average is 80%. Since the accuracies are close to the average, minimal bias is occurring.

Another method for validation has been performed using oversampling. The dataset size distribution is 92, 32, and 33 for mild/non-ASD, moderate and severe ASD groups, respectively. We have evaluated oversampling minority classes using synthetic minority oversampling technique (SMOTE). The idea of SMOTE is synthesizing new samples by selecting features that are close in the feature space, drawing a line between each couple of features and generating a new feature for a new sample at a point along that line. Similarly accuracy has been achieved after employing SMOTE, compared to accuracy obtained without rebalancing. The classification accuracy in classifying between mild and moderate is 78%, and the classification accuracy in classifying between mild and severe is 79%.

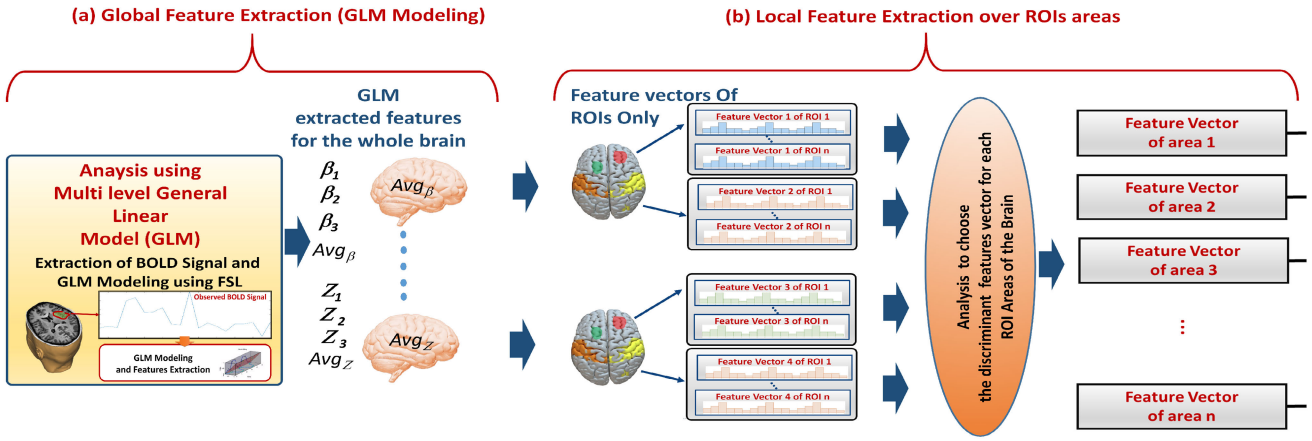

FIGURE 6. The pipeline for global (whole brain) and local (for each ROI) features extraction. We examine two GLM output files: 1) the average of the three GLM regressors representing the three audio stimuli, and 2) the average z-statistic of these regressors. Second, we perform local feature extraction by applying various calculations to the voxels included in each area to combine these features for each selected brain area.

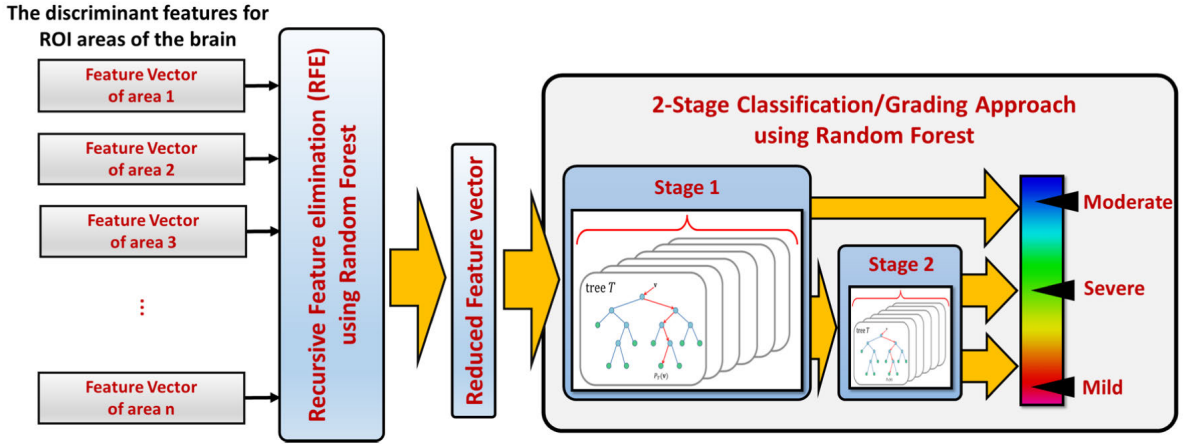

FIGURE 7. The pipeline of the severity grading approach. A two stage classification technique has been applied. First, each group is classified against the other groups. Second, a classification is applied between each pair of groups.

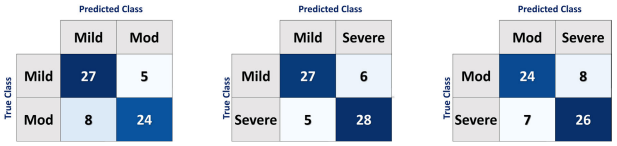

FIGURE 8. Confusion matrix of each balanced group pair.

V. DISCUSSION

In response to language tasks during sleep, infants and toddlers in those groups diagnosed with autism spectrum disorder showed hypoactivation of the bilateral primary auditory cortex, bilateral superior temporal gyrus, angular gyrus, and the cingulate gyrus. Whereas those within the mild group and non-ASD group showed typical left-sided dominance in response to a language task, this larger group of ASD subjects (those with moderate and severe ADOS CSS) showed a loss of this left hemisphere lateralization. These results in those toddler and infants who developed ASD is again consistent with the hypothesis that failure of proper language development and neural circuitry is an important indicator of autism and its severity [13], [15]–[18], [20]–[22]. We used multiple classification systems to delineate the mild/non-ASD groups from moderate and severe ASD groups with an average accuracy, sensitivity and specificity of 70% to 80%. Validation experiments further reinforce the reliability of our accuracy findings. Such simplistic language based task fMRI in sleeping infants and toddlers may lead to earlier identification of those at high risk for a psychology based diagnosis of ASD in the next 6–12 months. Earlier identification of those infants and toddlers can lead to earlier interventions and better long term developmental outcomes.

Analysis of this larger group of ASD infants and toddlers reinforces the hypothesis that this is a wide spread failure of typical language networks to develop in ASD. At 6–12 months, typically developed infants recruit both STG as well as frontal lobe motor areas [39] in response to auditory signals. In response to bedtime stories, 2 to 3 year

old typically developed toddlers show activation in the frontal, temporal, occipital, and cerebellar cortices [40]. Similarly, a language task based fMRI study in a smaller subset of the NDAR data suggests greater involvement of a widespread network including superior/inferior temporal cortices, anterior lateral and medial prefrontal cortex, amygdala/hippocampus/ventral striatum, anterior cingulate and insular cortices [15]. Likewise the same study, less activation was observed during the task involving segments of the thalamus, Crus IV, and V of the cerebellum, SMA, pre-SMA, motor/pre-motor areas, and the primary visual cortex.

Language development is thought to have a strong genetic component. Most measures of anatomical differences including enlarged WM tracts/thicker myelinated tracts, increased surface areas, larger pyramidal neurons, increased width of cortical columns, and increased afferent fiber contacts suggest a left predominant vs. right predominant language circuit during typical development [38], [39], [41]. Those with poor language outcomes in ASD have abnormal language developmental trajectory, as documented by their Mullen language scores, starting at 12 months and arriving at a nadir around 3 to 4 years of age [15]. Unlike that study [15], our results suggest significant impact of ASD groups severity on fMRI signaling not only in primary auditory cortex but also other ROIs examined in these experiments. There is at least moderate positive or negative correlations in language task-based MRI signals and behavioral language measures on the Mullen scales among ASD good and poor language outcome groups [15]. Thus, the cumulative data from language based task in at risk HR infants/toddlers with ASD, and older subjects suggest a hypothesis that developing language circuits may be a reasonable network to detect and assign ASD severity. These data are consistent with network efficiency studies which suggest that cortical-cortical organization are deficient in ASD in terms of both lower long range connectivity that provides rapid integration of information between different brain regions and aberrant spatial clustering/local connectivity that affects efficient processing of subtask information within a brain region [42].

The proposed framework achieves higher accuracies compared to our previous work which was performed on task-based fMRI scans of the same experiment. A direct comparison between our research and other literature would not be objective as other researches incorporate different data sets and task-based fMRI experiments. We achieve ASD grading accuracies reaching 84% on 157 subjects. To the best of our knowledge, literature of ASD diagnosis does not include research that achieves higher accuracies with this high number of subjects.

Our study has significant limitations which limit generalization. Other populations including those of global delay, language delay, TD groups, etc. may shed light on their contribution to fMRI signals in language circuits not specific to ASD. In addition, the response to speech spoken from live adults might be substantially different for awake infants/toddlers in comparison to a recorded speech. The incorporated fMRI studies have a relatively small sample size and lack a real control for variability that might exist in language circuits for this task and age across a population. These small samples sizes could also fail to detect small differences across groups or more complex developmental influences. States such as sleep stage may influence network activity. In the original report [13], sleep latency was not substantially different between groups and was felt not to impact fMRI signals.

From the methodological point of view, features extracted for classification are obtained from the statistical maps generated by GLM. Such features extract the temporal characteristics without correlation with spatial features. Our future work will focus on combining both spatial and temporal discriminant characteristics using wavelet transform [43] and artificial neural networks. Another limitation of GLM is that it assumes only linear relation between BOLD signals and the expected hemodynamic response. However, other nonlinear methods for correlation will be investigated.

The main contribution of our study is the whole system that extracts accurate discriminant features, based on the analysis of the brain functionality, and grades autism severity to locate subjects in the autism spectrum. We investigated our proposed feature extraction approach with the hypothesis that it obtains good results on several machine learning approaches. Therefore, we have chosen popular machine learning classifiers. After testing SVM, random forest and multi-layer perceptron, random forest achieves higher accuracies and fits the features. In future work, we will investigate more complex machine learning and deep learning classification approaches with multi-modal fusion to enhance grading accuracy.

In this report, the neural signals encoded in responses to speech at very young ages may not only predict later language abilities but may also place subjects very precisely along the autism spectrum. In general, social abilities usually track very closely with language abilities and one of the very typical hallmarks of autism is the impairment in social communication [44]. Our proof of concept results suggest that fMRI signals in language circuits may be a very good marker for ASD and/or autism severity. Previous studies suggest a multi-modal approach may lead to more accurate classification [15]. These modalities may include the transcriptome, ERP/EEG, MEG, fNIRs, and DTI/Rs/Structural MRI [13]–[18], [20]–[22]. Such works need to combine evidence of MRI modalities, genetics, and early clinical behavioral assessment in larger sample sizes where the prevalence of ASD subgroups could be accurately quantitated. Such classification would also need to include non ASD populations such as larger sample size of TD group, global developmental delay group, and language delayed groups [13]. In this study, our classification system using local and global features with ROIs in language circuits gives an accurate classification in a larger group of infants/toddlers of 75% to 84% depending upon the experiment. Cross validation and multiple comparisons during experiments lends credence to our original

results using our classifiers. A plethora of previous studies support our current data [13]–[18], [20]–[22].

As more accurate methodologies to map multiple behavioral traits onto neurobiological substrates becomes available, we are closer to our goal to individually assess the biology of the patient in clinic, anticipate phenotypes, and more importantly prescribe personalized treatments/medicines.

REFERENCES

[1] Autism Speaks, "Autism and health: A special report by autism speaks," Tech. Rep., 2019, pp. 2018–2109, vol. 19.
[2] K. Gotham, A. Pickles, and C. Lord, "Trajectories of autism severity in children using standardized ADOS scores," *Pediatrics*, vol. 130, no. 5, pp. e1278–e1284, 2012.
[3] C. Lord, M. Elsabbagh, G. Baird, and J. Veenstra-Vanderweele, "Autism spectrum disorder," *Lancet*, vol. 392, no. 10146, pp. 508–520, 2018.
[4] K. Gotham, A. Pickles, and C. Lord, "Standardizing ADOS scores for a measure of severity in autism spectrum disorders," *J. Autism Develop. Disorders*, vol. 39, no. 5, pp. 693–705, May 2009.
[5] J. Blume, K. Wittke, L. Naigles, and A. M. Mastergeorge, "Language growth in young children with autism: Interactions between language production and social communication," *J. Autism Develop. Disorders*, vol. 51, no. 2, pp. 644–665, Feb. 2021.
[6] R. Stoner, M. L. Chow, M. P. Boyle, S. M. Sunkin, P. R. Mouton, S. Roy, A. Wynshaw-Boris, S. A. Colamarino, E. S. Lein, and E. Courchesne, "Patches of disorganization in the neocortex of children with autism," *New England J. Med.*, vol. 370, no. 13, pp. 1209–1219, Mar. 2014.
[7] M. F. Casanova, A. El-Baz, and J. S. Suri, *Autism Imaging and Devices*. Boca Raton, FL, USA: CRC Press, 2017.
[8] K. Pierce, V. H. Gazestani, E. Bacon, C. C. Barnes, D. Cha, S. Nalabolu, L. Lopez, A. Moore, S. Pence-Stophaeros, and E. Courchesne, "Evaluation of the diagnostic stability of the early autism spectrum disorder phenotype in the general population starting at 12 months," *JAMA Pediatrics*, vol. 173, no. 6, pp. 578–587, 2019.
[9] M. M. T. Ismail, "A CAD system for early diagnosis of autism using different imaging modalities," Ph.D. dissertation, Dept. Elect. Comput. Eng., Univ. Louisville, Louisville, KY, USA, 2016.
[10] K. J. Friston, "Modalities, modes, and models in functional neuroimaging," *Science*, vol. 326, no. 5951, pp. 399–403, Oct. 2009.
[11] J. S. Anderson, M. A. Ferguson, and J. A. Nielsen, "Functional MRI in autism," in *Imaging the Brain in Autism*, M. F. Casanova, A. S. El-Baz, and J. Suri, Eds. New York, NY, USA: Springer, 2013, pp. 289–324.
[12] A. J. Herringshaw, C. J. Ammons, T. P. DeRamus, and R. K. Kana, "Hemispheric differences in language processing in autism spectrum disorders: A meta-analysis of neuroimaging studies," *Autism Res.*, vol. 9, no. 10, pp. 1046–1057, Oct. 2016.
[13] L. T. Eyler, K. Pierce, and E. Courchesne, "A failure of left temporal cortex to specialize for language is an early emerging and fundamental property of autism," *Brain*, vol. 135, no. 3, pp. 949–960, Mar. 2012.
[14] M. V. Lombardo, T. Pramparo, V. Gazestani, V. Warrier, R. A. I. Bethlehem, C. C. Barnes, L. Lopez, N. E. Lewis, L. Eyler, K. Pierce, and E. Courchesne, "Large-scale associations between the leukocyte transcriptome and BOLD responses to speech differ in autism early language outcome subtypes," *Nature Neurosci.*, vol. 21, no. 12, p. 1680, 2018.
[15] M. V. Lombardo, K. Pierce, L. T. Eyler, C. C. Barnes, C. Ahrens-Barbeau, S. Solso, K. Campbell, and E. Courchesne, "Different functional neural substrates for good and poor language outcome in autism," *Neuron*, vol. 86, no. 2, pp. 567–577, Apr. 2015.
[16] A. K. Lindell and K. Hudry, "Atypicalities in cortical structure, handedness, and functional lateralization for language in autism spectrum disorders," *Neuropsychol. Rev.*, vol. 23, pp. 257–270, Sep. 2013.
[17] A. M. Seery, V. Vogel-Farley, H. Tager-Flusberg, and C. A. Nelson, "Atypical lateralization of ERP response to native and non-native speech in infants at risk for autism spectrum disorder," *Develop. Cognit. Neurosci.*, vol. 5, pp. 10–24, Jul. 2013.
[18] M. Mody, D. S. Manoach, F. H. Guenther, T. Kenet, K. A. Bruno, C. J. McDougle, and K. A. Stigler, "Speech and language in autism spectrum disorder: A view through the lens of behavior and brain imaging," *Neuropsychiatry*, vol. 3, no. 2, p. 223, 2013.
[19] R. C. M. Philip, M. R. Dauvermann, H. C. Whalley, K. Baynham, S. M. Lawrie, and A. C. Stanfield, "A systematic review and meta-analysis of the fMRI investigation of autism spectrum disorders," *Neurosci. Biobehav. Rev.*, vol. 36, no. 2, pp. 901–942, Feb. 2012.
[20] G. Lai, H. D. Schneider, J. C. Schwarzenberger, and J. Hirsch, "Speech stimulation during functional MR imaging as a potential indicator of autism," *Radiology*, vol. 260, no. 2, pp. 521–530, Aug. 2011.
[21] A. Karten and J. Hirsch, "Brief report: Anomalous neural deactivations and functional connectivity during receptive language in autism spectrum disorder: A functional MRI study," *J. Autism Develop. Disorders*, vol. 45, no. 6, pp. 1905–1914, Jun. 2015.
[22] E. A. Kliuev, G. E. Sheyko, M. G. Dunayev, S. A. Abramov, V. V. Dvoryaninova, O. V. Balandina, N. N. Karyakin, and A. N. Belova, "The role of functional MRI in understanding the origin of speech delay in autism spectrum disorders," *Sovremennye tehnologii v Med.*, vol. 11, no. 3, p. 66, Sep. 2019.
[23] O. Dekhil, M. Ali, Y. El-Nakieb, A. Shalaby, A. Soliman, A. Switala, A. Mahmoud, M. Ghazal, H. Hajjdiab, M. F. Casanova, A. Elmaghraby, R. Keynton, A. El-Baz, and G. Barnes, "A personalized autism diagnosis CAD system using a fusion of structural MRI and resting-state functional MRI data," *Frontiers Psychiatry*, vol. 10, p. 392, Jul. 2019, doi: 10.3389/fpsyt.2019.00392.
[24] G. Chanel, S. Pichon, L. Conty, S. Berthoz, C. Chevallier, and J. Grèzes, "Classification of autistic individuals and controls using cross-task characterization of fMRI activity," *NeuroImage, Clin.*, vol. 10, pp. 78–88, Jan. 2016.
[25] N. C. Dvornek, D. Yang, P. Ventola, and J. S. Duncan, "Learning generalizable recurrent neural networks from small task-fMRI datasets," in *Proc. Int. Conf. Med. Image Comput. Comput.-Assist. Intervent.* New York, NY, USA: Springer, 2018, pp. 329–337.
[26] X. Li, N. C. Dvornek, X. Papademetris, J. Zhuang, L. H. Staib, P. Ventola, and J. S. Duncan, "2-channel convolutional 3D deep neural network (2CC3D) for fMRI analysis: ASD classification and feature learning," in *Proc. IEEE 15th Int. Symp. Biomed. Imag. (ISBI)*, Apr. 2018, pp. 1252–1255.
[27] J. Zhuang, N. C. Dvornek, X. Li, D. Yang, P. Ventola, and J. S. Duncan, "Prediction of pivotal response treatment outcome with task fMRI using random forest and variable selection," in *Proc. IEEE 15th Int. Symp. Biomed. Imag. (ISBI)*, Apr. 2018, pp. 97–100.
[28] R. Haweel, O. Dekhil, A. Shalaby, A. Mahmoud, M. Ghazal, R. Keynton, G. Barnes, and A. El-Baz, "A machine learning approach for grading autism severity levels using task-based functional MRI," in *Proc. IEEE Int. Conf. Imag. Syst. Techn. (IST)*, Abu Dhabi, UAE, Dec. 2019, pp. 1–5.
[29] R. Haweel, O. Dekhil, A. Shalaby, A. Mahmoud, M. Ghazal, A. Khalil, R. Keynton, G. Barnes, and A. El-Baz, "A novel framework for grading autism severity using task-based FMRI," in *Proc. IEEE 17th Int. Symp. Biomed. Imag. (ISBI)*, Apr. 2020, pp. 1404–1407.
[30] M. W. Woolrich, B. D. Ripley, M. Brady, and S. M. Smith, "Temporal autocorrelation in univariate linear modeling of FMRI data," *NeuroImage*, vol. 14, no. 6, pp. 1370–1386, Dec. 2001.
[31] M. Jenkinson, C. F. Beckmann, T. E. Behrens, M. W. Woolrich, and S. M. Smith, "FSL," *NeuroImage*, vol. 62, no. 2, pp. 782–790, 2012.
[32] M. Jenkinson, P. Bannister, M. Brady, and S. Smith, "Improved optimization for the robust and accurate linear registration and motion correction of brain images," *NeuroImage*, vol. 17, no. 2, pp. 825–841, Oct. 2002.
[33] J. L. Lancaster, D. Tordesillas-Gutiérrez, M. Martinez, F. Salinas, A. Evans, K. Zilles, J. C. Mazziotta, and P. T. Fox, "Bias between MNI and talairach coordinates analyzed using the ICBM-152 brain template," *Hum. Brain Mapping*, vol. 28, no. 11, pp. 1194–1205, 2007. [Online]. Available: https://onlinelibrary.wiley.com/doi/abs/10.1002/hbm.20345
[34] C. F. Beckmann, M. Jenkinson, and S. M. Smith, "General multilevel linear modeling for group analysis in FMRI," *NeuroImage*, vol. 20, no. 2, pp. 1052–1063, 2003.
[35] Y. Zang, T. Jiang, Y. Lu, Y. He, and L. Tian, "Regional homogeneity approach to fMRI data analysis," *NeuroImage*, vol. 22, no. 1, pp. 394–400, May 2004.
[36] M. W. Woolrich, T. E. J. Behrens, C. F. Beckmann, M. Jenkinson, and S. M. Smith, "Multilevel linear modelling for FMRI group analysis using Bayesian inference," *NeuroImage*, vol. 21, no. 4, pp. 1732–1747, 2004.
[37] P. M. Granitto, C. Furlanello, F. Biasioli, and F. Gasperi, "Recursive feature elimination with random forest for PTR-MS analysis of agroindustrial products," *Chemometric Intell. Lab. Syst.*, vol. 83, no. 2, pp. 83–90, Sep. 2006.

[38] S. Solso, R. Xu, J. Proudfoot, D. J. Hagler, K. Campbell, V. Venkatraman, C. Carter Barnes, C. Ahrens-Barbeau, K. Pierce, A. Dale, L. Eyler, and E. Courchesne, "Diffusion tensor imaging provides evidence of possible axonal overconnectivity in frontal lobes in autism spectrum disorder toddlers," *Biol. Psychiatry*, vol. 79, no. 8, pp. 676–684, Apr. 2016.
[39] M. Majorano, M. M. Vihman, and R. A. DePaolis, "The relationship between infants' production experience and their processing of speech," *Lang. Learn. Develop.*, vol. 10, no. 2, pp. 179–204, Apr. 2014.
[40] E. Redcay and E. Courchesne, "Deviant functional magnetic resonance imaging patterns of brain activity to speech in 2–3-year-old children with autism spectrum disorder," *Biol. Psychiatry*, vol. 64, no. 7, pp. 589–598, Oct. 2008.
[41] E. Courchesne, T. Pramparo, V. H. Gazestani, M. V. Lombardo, K. Pierce, and N. E. Lewis, "The ASD living biology: From cell proliferation to clinical phenotype," *Mol. Psychiatry*, vol. 24, no. 1, pp. 88–107, Jan. 2019.
[42] J. D. Lewis, A. C. Evans, J. R. Pruett, K. Botteron, L. Zwaigenbaum, A. Estes, G. Gerig, L. Collins, P. Kostopoulos, R. McKinstry, S. Dager, S. Paterson, R. T. Schultz, M. Styner, H. Hazlett, and J. Piven, "Network inefficiencies in autism spectrum disorder at 24 months," *Transl. Psychiatry*, vol. 4, no. 5, p. e388, May 2014.
[43] A. Bernas, A. P. Aldenkamp, and S. Zinger, "Wavelet coherence-based classifier: A resting-state functional MRI study on neurodynamics in adolescents with high-functioning autism," *Comput. Methods Programs Biomed.*, vol. 154, pp. 143–151, Feb. 2018.
[44] A. D. Friederici and K. Alter, "Lateralization of auditory language functions: A dynamic dual pathway model," *Brain Lang.*, vol. 89, no. 2, pp. 267–276, May 2004.

REEM HAWEEL received the B.Sc. and M.S. degrees in computer systems from the Faculty of Information and Computer Sciences, Ain Shams University, Cairo, Egypt. She is currently pursuing the Ph.D. degree in computer systems and bioengineering.

In November 2018, she has joined the BioImaging Laboratory, University of Louisville, Louisville, KY, USA, as a Graduate Research Assistant. She has been a Lecturer Assistant at the Faculty of Information and Computer Sciences, Ain Shams University, since 2010. Her research interests include medical image analysis, big data, machine learning, artificial intelligence, and parallel computing. Her current research interests include developing new computer aided diagnostic (CAD) systems for autism diagnosis with task fMRI, resting fMRI, and DTI images.

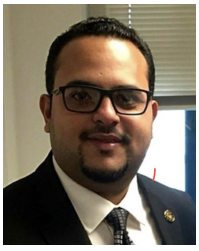

AHMED M. SHALABY received the B.S. and M.S. degrees in electrical engineering from Alexandria University, Egypt, in 2003 and 2009, respectively, and the Ph.D. degree in electrical engineering from the University of Louisville, Louisville, USA, in 2014.

He is currently working as a Postdoctoral Research Associate at the Bioengineering Department, University of Louisville. His research interests include computer vision and image processing, object detection and tracking, medical imaging, and facial biometrics.

ALI H. MAHMOUD received the B.S. and M.S. degrees in electrical engineering from Alexandria University, Egypt, in 2005 and 2009, respectively, and the Ph.D. degree in electrical engineering from the University of Louisville, Louisville, USA, in 2014.

He is currently working as a Postdoctoral Research Associate at the Bioengineering Department, University of Louisville. His research interests include computer vision and image processing, object detection and tracking, medical imaging, and facial biometrics.

MOHAMMED GHAZAL (Senior Member, IEEE) received the B.Sc. degree in computer engineering from the American University of Sharjah and the M.S. and Ph.D. degrees in electrical and computer engineering (ECE) from Concordia University, Canada, in 2006 and 2010, respectively. He is currently an Associate Professor of ECE and the Chair of a department at Abu Dhabi University (ADU). He lead the B.Sc. programs in ECE to achieve ABET and WASC accreditation. He also leads ADU E-Learning initiative. He has authored over 50 publications in technical journals and international conferences, including *Renewable and Sustainable Energy Reviews* (Elsevier), IEEE TRANSACTIONS ON IMAGE PROCESSING, IEEE TRANSACTIONS ON CIRCUITS AND SYSTEMS FOR VIDEO TECHNOLOGY, and IEEE TRANSACTIONS ON CONSUMER ELECTRONICS. His current research interests include biomedical signal processing, mobile computing, and embedded systems. He is a member of the ACM and the BMES. He was awarded the Alexander Graham Bell Fellowship by NSERC and the QFRNT by the Government of Quebec. He was also awarded the President's Cup and the Ministry of Education Shield for Creative Thinking at the American University of Sharjah. During his time at ADU, he received multiple awards, including the University Teaching Award, in 2013, and the Distinguished Faculty Award, in 2014 and 2016.

NOHA SEADA received the B.Sc., M.S., and Ph.D. degrees in scientific computing from the Faculty of Computer and Information, Ain Shams University, Cairo, Egypt, in 2004, 2009, and 2017, respectively. She worked for six years as a Senior Developer and promoted to Team Leader for developing non-invasive computer aided diagnosis software at Healthy-IT Company. She is currently working as a Lecturer and a Postdoctoral Researcher at the Computer Systems Department, Faculty of Computer and Information, Ain Shams University. Her research interests include medical image analysis, computer vision, machine learning, deep learning, human activity recognition, and artificial intelligence. In 2011, she was awarded the Google Anita Borg Memorial Scholarship for Europe, Middle East, and Africa. In 2013, she was awarded a scholarship for joining the Vision and Image Processing Laboratory, Waterloo University, Canada, for conducting part of her Ph.D. Research.

SAID GHONIEMY received the Ph.D. degree in computer engineering from the "Institut National Polytechnique de Toulouse," France, in 1982. He is currently a Professor with the Department of Computer Systems, Faculty of Computers and Information Sciences, Ain Shams University, Cairo, Egypt. He supervised more than 40 Ph.D. and M.Sc. thesis, and coauthored over 80 publications in the areas of computer systems, signal and image processing, robotics and computer vision, and mobile *ad-hoc* networks.

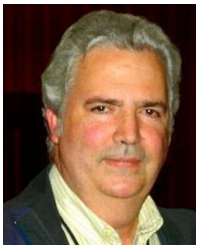

MANUEL CASANOVA is the SmartState Endowed Chair of the Childhood Neurotherapeutics and a Professor of biomedical sciences at the University of South Carolina School of Medicine Greenville. He is the former Gottfried and Gisela Kolb Endowed Chair of outpatient psychiatry and a Professor of anatomical sciences and neurobiology at the University of Louisville. His neuromorphology research, conducted in collaboration with other researchers from around the globe, has found there are drastic differences in the brains of autistic individuals. The studies that he conducted show that minicolumns (or brain strands) of autism spectrum individuals have more cells, but they are narrower and more densely packed, which he says can limit the brain's ability to send messages. He claimed this helps explain symptoms since "there's not enough juice to actually power very long connections in the brain."

GREGORY N. BARNES is the Inaugural Permanent Director of the University of Louisville Autism Center. He also holds the Spafford Ackerly Chair of child and adolescent psychiatry and a Faculty Member positions with the Departments of Neurology and Pediatrics. His research interests include potential genetic influences into the development of ASD and epilepsy and how these factors contribute to outcomes and potential new treatments. He is a UL Professor of neurology and pediatrics and has held academic appointments at the Washington University School of Medicine, St. Louis; the Harvard Medical School; the Duke University Medical School; the University of Kentucky College of Medicine; and the Vanderbilt School of Medicine. He has authored or coauthored 58 research articles/book chapters in the fields of neurology, autism, and epilepsy. He currently serves as the PI of several national multi-site grants to understand the role of cannabinoid signaling in autism.

AYMAN EL-BAZ (Senior Member, IEEE) received the B.Sc. and M.Sc. degrees in electrical engineering, in 1997 and 2001, respectively, and the Ph.D. degree in electrical engineering from the University of Louisville, in 2006. He is a Distinguished Professor, a University Scholar, and the Chair of the Bioengineering Department, University of Louisville, KY, USA. In 2009, he was named a Coulter Fellow for his contributions to the field of biomedical translational research. He has 17 years of hands-on experience in the fields of bio-imaging modeling and non-invasive computer-assisted diagnosis systems. He has authored or coauthored more than 500 technical articles (145 journals, 27 books, 78 book chapters, 225 refereed-conference papers, 172 abstracts, and 30 U.S. patents and disclosures).